

Supplementary Information

Filippo Federici Canova,^{*a} Masashi Mizukami,^b Takako Imamura,^b Kazue Kurihara^{a,b}
and Alexander L. Shluger^{a,c}

Received Xth XXXXXXXXXXXX 20XX, Accepted Xth XXXXXXXXXXXX 20XX

First published on the web Xth XXXXXXXXXXXX 20XX

DOI: 10.1039/b000000x

1 Creating a-SiO₂+H surfaces

Amorphous SiO₂ was obtained by melting a stoichiometric cristobalite bulk, consisting of 9600 atoms, at 4000 K and atmospheric pressure. After being equilibrated for 0.5 ns, the fluid was cooled down to room temperature (cooling rate 3.7 K/ps), and equilibrated again for 1 ns. We used BKS to treat interatomic interactions¹, since it is known to reproduce the properties of a-SiO₂ quite well. Given the large size of the system, compared to the original BKS study cases, we used particle-particle-particle-mesh² to treat electrostatic interactions, rather than Ewald summation. Due to the delicate balance between long- and short-range interactions, we could not replicate the BKS results with modern methods, and noticed how the obtained glass density depends on the interaction cutoff r_c . Therefore we set $r_c = 0.7$ nm, giving the bulk density $\rho = 2.34$ g/cm³, expected of BKS.

After cooling, the force field was changed to ClayFF³, since it includes the description of SiOH lacking in BKS. However, BKS was chosen to produce the amorphous bulk since it gives structures that better agree with experiments. Stoichiometric slabs, with a surface area of 5.165×5.165 nm² and thickness 1.5 nm, were cut from the bulk and relaxed for 1 ns at room temperature. Despite the smaller partial charges of ClayFF, the slabs did not show significant deformation after relaxation. However, the surfaces contained abundant defects such as three-coordinated Si and dangling O. We then passivated the defects of different type located within a given depth d_{def} from the two surfaces, by manually splitting H₂O according to the following procedure, until 4.6 OH/nm² were present in the system.

(1) First we detected 3-coordinated Si and dangling O. These were passivated with OH and H respectively, adding two isolated (rarely vicinal) SiOH.

(2) Si atoms bound to two bridging O and one dangling O, are simultaneously OH and H acceptors. These defects are present in low concentration (0.04 OH/nm²), and when passivated, produce a geminal site with two SiOH groups.

(3) Then we located pairs of Si atoms directly connected by two O (M2 rings), and broke one of the connections, leaving a 3-coordinated Si and a dangling O. These act as OH and H acceptors respectively, adding two vicinal SiOH groups to the surface.

(4) Additional H-OH acceptors were created by randomly breaking Si-O-Si bridges on the surfaces, until the desired density of 4.6 OH/nm² was reached. This way, isolated, vicinal and geminal sites can be obtained. In practice, the slabs had enough defects that after steps (1) and (2), about 3 OH/nm² were already present on the surfaces, and (4) adds mostly vicinal groups.

Given the simplicity of the force fields (BKS and ClayFF), creation and hydroxylation of a-SiO₂ were

performed with the HOOMD-blue code^{4,5*}, taking advantage of the massively parallel GPU architecture.

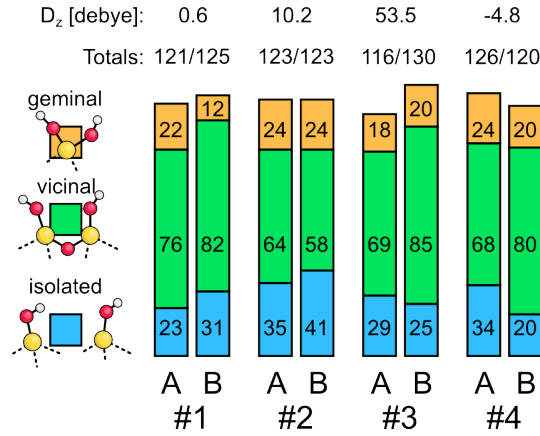


Fig. 1 (Colour online) Amount of isolated (blue), vicinal (green) and geminal (orange) silanol groups in the final surfaces. The chart also shows the amount of SiOH on each side of the slabs, and the component of their dipole normal to the surface xy plane.

This procedure was repeated for different melts, generating 4 slabs with a total of 246 SiOH groups on the two surfaces. No constraint was applied in order to ensure an equal amount of SiOH on each surface of the slabs, thus small differences can be seen (Fig. 1). Since most of the SiOH originate from defects already present on the surfaces, we cannot entirely control the proportion of isolated, vicinal and geminal groups. However, the majority are vicinal, as expected from experiments⁶. Breaking bridges as done in (4) can also remove the common Si-O-Si between two adjacent SiO rings, forming an apparent, larger ring on the surface, and leading to atomic scale roughness. The distribution of SiOH groups on the α -SiO₂ surfaces is not homogeneous, as shown in Fig. 1 of the manuscript, and occasionally appear inside the large holes, or even deeper in the slab.

As mentioned earlier, only defects within a depth d_{def} from the two surfaces were considered as H-OH acceptors. When hydroxylating slabs #1 and #2, d_{def} was set to the thickness of the slab, thus passivating all

| slab # | Si-4O | Si-3O | Si-2O |
|--------|-------|-------|-------|
| 1 | 100 | 0 | 0 |
| 2 | 100 | 0 | 0 |
| 3 | 98.4 | 1.5 | 0.1 |
| 4 | 99.5 | 0.5 | 0 |

Table 1 Amount (%) of 4-,3- and 2-coordinated Si in the slabs.

defects (Table 1). Since deprotonation of SiOH is expected to occur in real systems, a small surface charge is expected. However, our simulation cannot treat dissociation of SiOH, nor a net charge in the system. For these reasons, we created defective slabs. This was achieved by setting the search dept d_{def} for defects to 0.5 nm for slab #3, leaving 14 (1.5%) of 3-coordinated Si, one 2-coordinated Si, and the corresponding amount of dangling O. In slab #4 we set $d_{def} = 0.7$ nm, giving only 5 (0.5%) 3-coordinated Si.

The electric field above the slabs varies greatly for our samples. In order to quantify it, we use the component of the dipole D_z normal to the surface plane, which, unlike the electric field, it is an intrinsic property of the slabs and does not depend on the position where it is calculated. (Fig. 1). Despite being created in the same way, #1 shows almost no polarisation, while #2 has a vertical dipole of 10.2 Debye.

* <http://codeblue.umich.edu/hoomd-blue>

Since the two slabs were prepared in the same way, and were fully passivated, the different D_z comes from the atomic configuration. Therefore, such polarisation can be expected, locally, on macroscopic silica surfaces. It appears that non-passivated defects contribute to higher dipole, as seen in slab #3. However, in small amount, such as in #4, we cannot see their effect, since the dipole is comparable to the ones of defect-free slabs #1 and #2.

2 Ionic liquid films

2.1 Structure

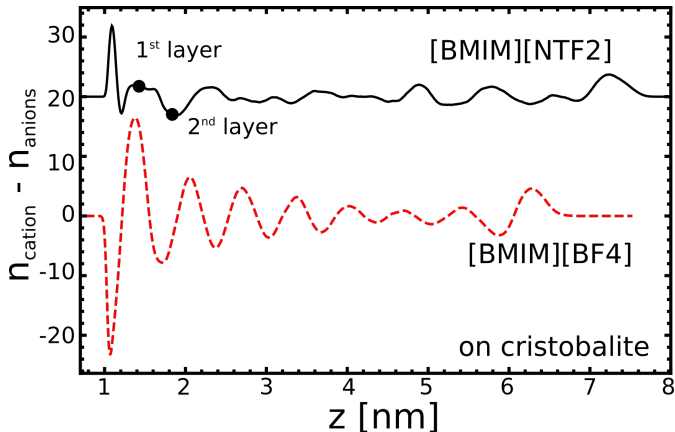


Fig. 2 (Colour online) Number density profiles showing the cumulative difference between cations and anions calculated for [BMIM][NTF2] (black) and [BMIM][BF4] (dashed red) on cristobalite. The markers for [BMIM][NTF2] are located at the edge of the first and second layer of the liquid.

Figure 2 shows the cumulative cation/anion imbalance throughout the IL films on cristobalite. Large oscillations are seen for [BMIM][BF4] (red line), corresponding to the alternated layers. In the first layers, the disparity reaches 20 ions, it decreases further from the surface, and finally appears again at the liquid-vacuum interface. For [BMIM][NTF2], we observe a high mismatch of 10 ions in proximity of the surface, since [NTF2] adsorbs slightly closer than [BMIM]. However, when the overall first layer is considered (see marker in Fig. 2), only 1-2 cations are in excess. The layers appear effectively neutral. At the liquid-vacuum interface we observe oscillations.

On a-SiO₂ surfaces, the trend is similar to the crystal case, for both liquids, but the mismatch is always smaller. From Fig. 3 we can observe how strongly polar surfaces can affect the layered structure. The electric field on surface #3A is strong enough to attract excess [NTF2] close to the surface. This is also seen on #4B to a lesser degree, which also has positive and smaller D_z . However the same behaviour is not observed on #1A, which has stronger dipole than #4B, indicating that the fine structural details of the surface are more important in determining the structure of the solid-liquid interface. Only stronger fields can make a difference in proximity of the surface. With [BMIM][BF4], the boundary layer is always anion rich, regardless of the surface, although a small positive kink is at the interface with #3B. There, the strong polarisation can push some anions away, leaving few cations in excess.

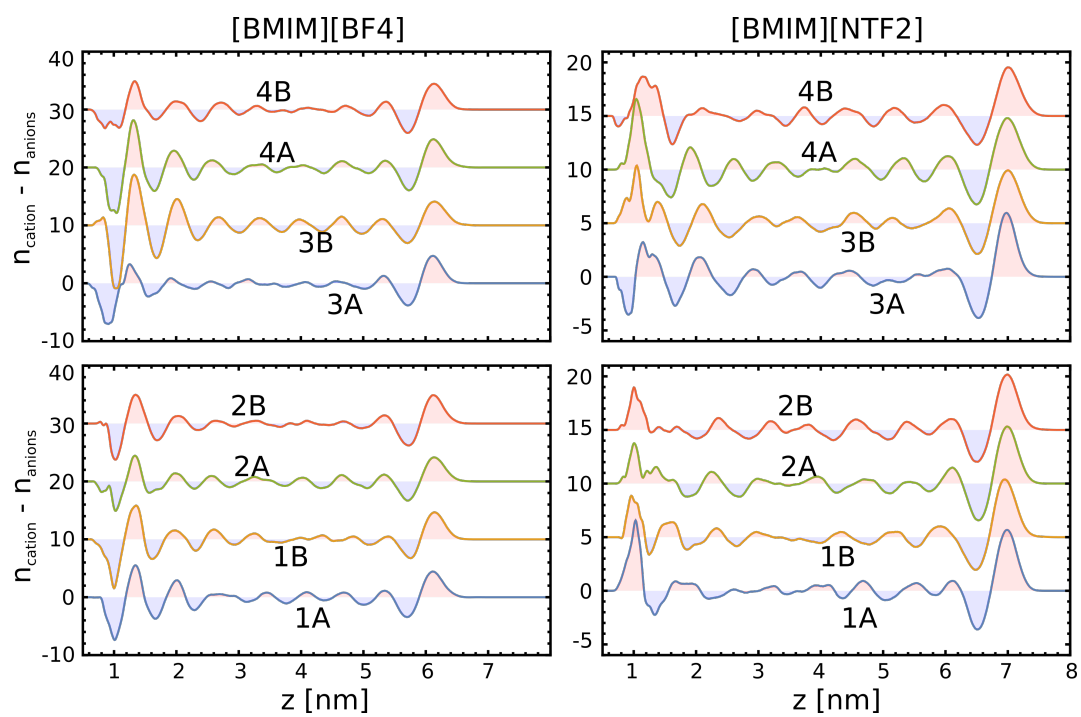


Fig. 3 (Colour online) Number density profiles showing the cumulative difference between cations and anions calculated for [BMIM][NTF2] (left) and [BMIM][BF4] (right) on a-SiO₂ surfaces. Each line is offset to avoid overlaps. The red/blue shading under the lines are a guide for the eye, indicating when the value is positive or negative respectively.

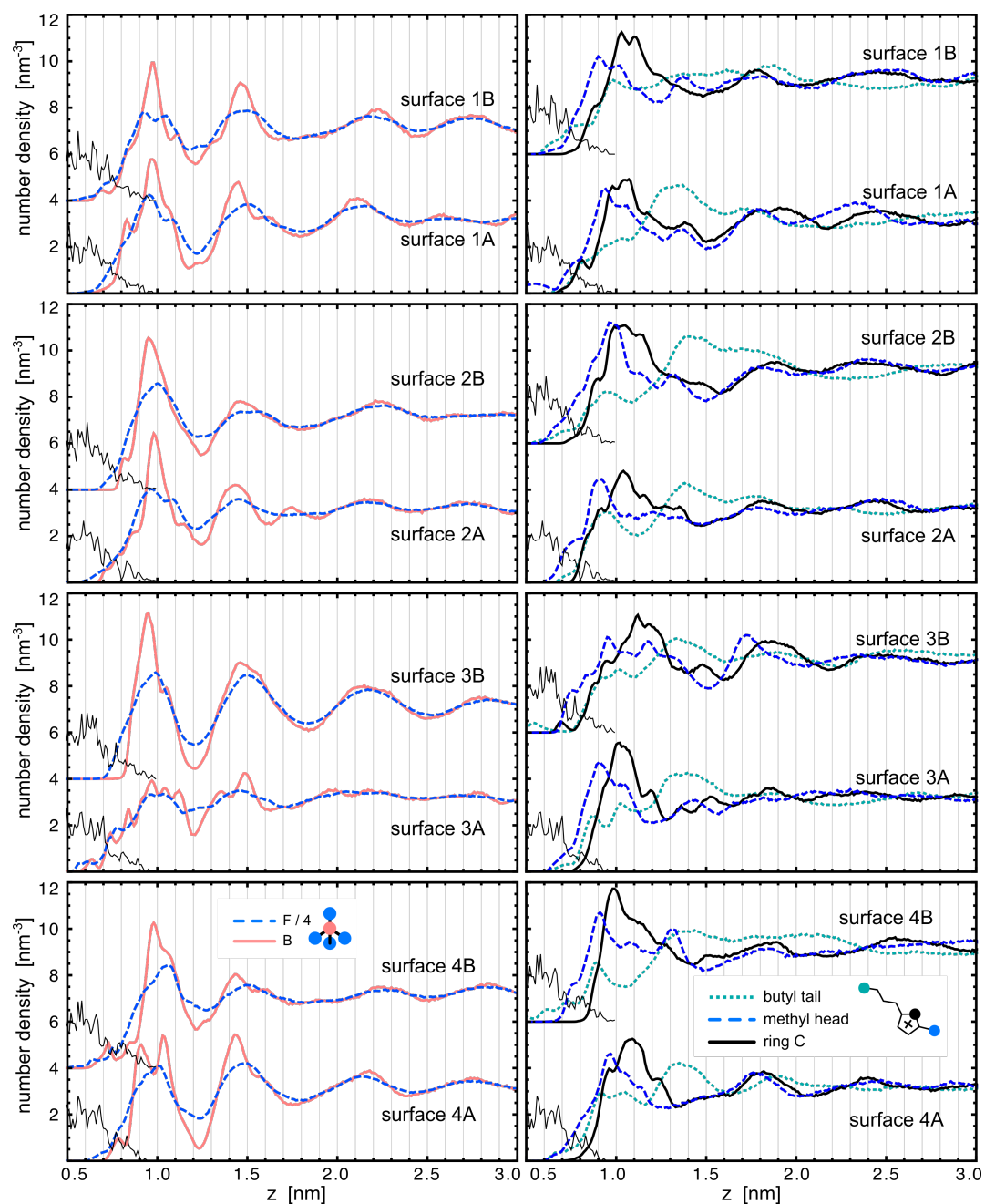


Fig. 4 (Colour online) Atomic density profiles for [BMIM][BF₄] anions (left) and cations (right) on a-SiO₂ surfaces. Solid pink line represents density of B, while dashed blue lines show the density of F atoms (normalised according to the stoichiometry). For cations, profiles for methyl heads, central ring C, and butyl terminations are shown by dashed blue, solid black, and dotted cyan lines respectively. Thin black lines represent the density of O from silica (scaled down by a factor of 25). In all plots, the profiles for side B of each surface were offset to improve readability.

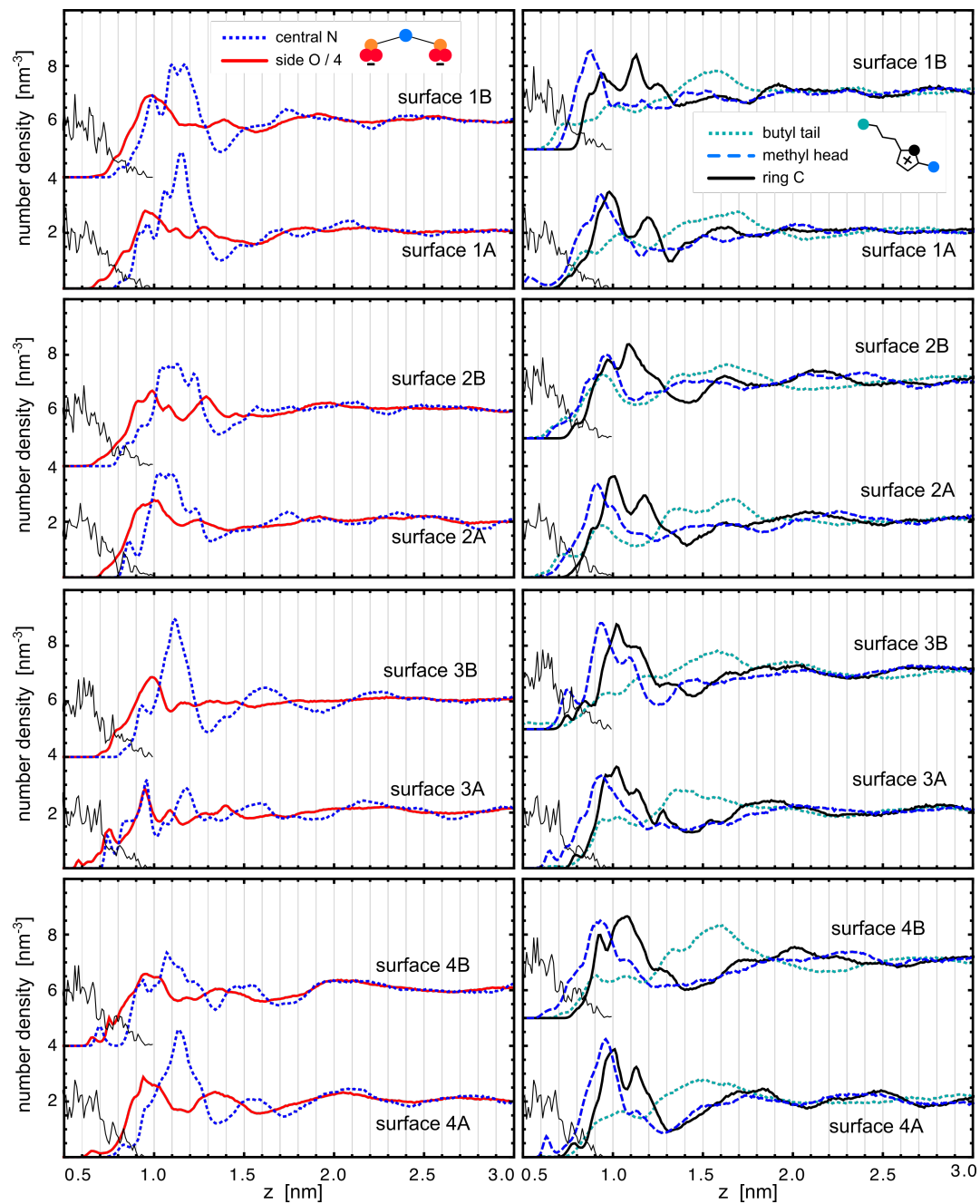


Fig. 5 (Colour online) Atomic density profiles for [BMIM][NTF2] anions (left) and cations (right) on a-SiO₂ surfaces. Solid red line represents density of O (normalised according to the stoichiometry), while dashed blue lines show the density of N atoms in anions. For cations, profiles for methyl heads, central ring C, and butyl terminations are shown by dashed blue, solid black, and dotted cyan lines respectively. Thin black lines represent the density of O from silica (scaled down by a factor of 25). In all plots, the profiles for side B of each surface were offset to improve readability.

2.2 Charges

Charge density profiles for [BMIM][BF₄] and [BMIM][NTF₂] on all amorphous silica surfaces are shown in Fig. 6 and Fig. 7 respectively.

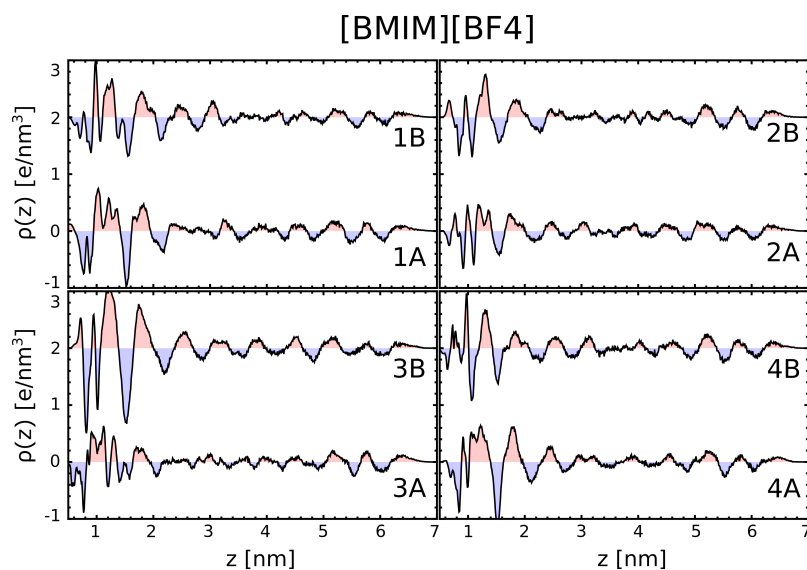


Fig. 6 (Colour online) Charge density profiles for [BMIM][BF₄] on a-SiO₂ surfaces. The red/blue shading under each line is a guide for the eye to distinguish regions of positive and negative charge respectively. In all plots, the profile for the liquid on surface side B is offset by 2 e/nm^3 to improve readability.

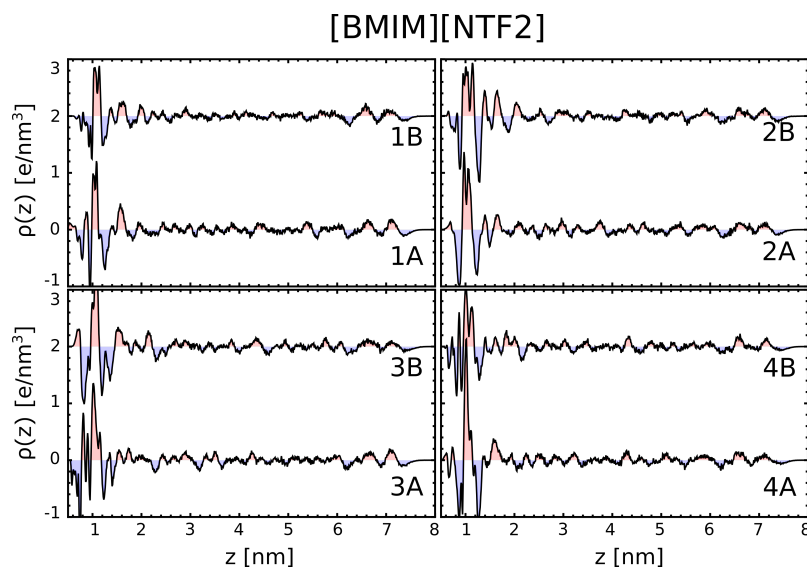


Fig. 7 (Colour online) Charge density profiles for [BMIM][NTF₂] on a-SiO₂ surfaces. The red/blue shading under each line is a guide for the eye to distinguish regions of positive and negative charge respectively. In all plots, the profile for the liquid on surface side B is offset by 2 e/nm^3 to improve readability.

3 Bulk liquids

We simulated the two bulk liquids in order to compare their equilibrium structure to the ones observed on silica surfaces. The bulk simulations were performed with 500 molecular pairs, in the NPT ensemble (1 and 300 K). Figure 8 shows the radial distribution function for anions and methyl, central C, and butyl

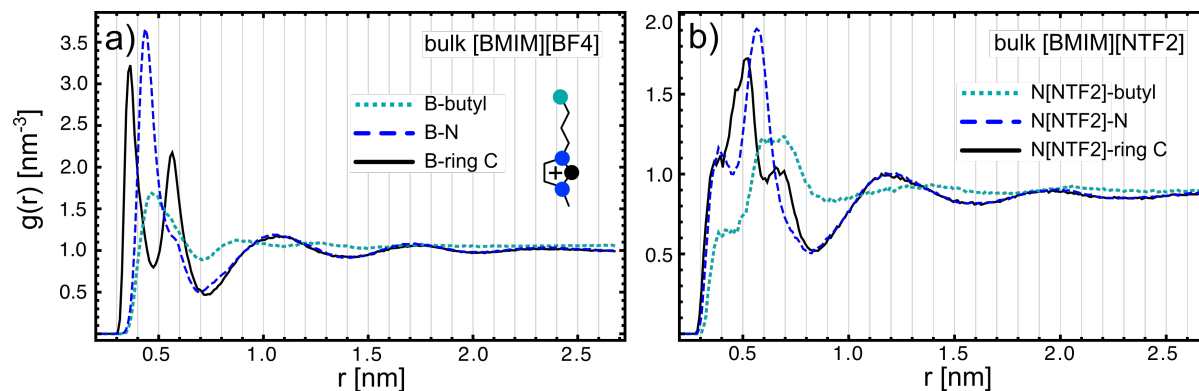


Fig. 8 (Colour online) Normalised radial distribution function for anion-cation distances in bulk (a) [BMIM][BF₄] and (b) [BMIM][NTF₂]. B atom is chosen as centre of [BF₄] while the central N is used for [NTF₂].

species in the cations. B is chosen as centre of [BF₄], while N for [NTF₂].

References

- 1 B. W. H. van Beest, G. J. Kramer and R. A. van Santen, *Physical Review Letters*, 1990, **64**, 1955–1958.
- 2 R. W. Hockney and J. W. Eastwood, *Computer simulation using particles*, Taylor & Francis, Inc., Bristol, PA, USA, 1988.
- 3 R. T. Cygan, J.-J. Liang and A. G. Kalinichev, *Journal of Physical Chemistry B*, 2004, **108**, 1255–1266.
- 4 J. A. Anderson, C. D. Lorenz and A. Travesset, *Journal of Computational Physics*, 2008, **227**, 5342 – 5359.
- 5 D. N. LeBard, B. G. Levine, P. Mertmann, S. A. Barr, A. Jusufi, S. Sanders, M. L. Klein and A. Z. Panagiotopoulos, *Soft Matter*, 2012, **8**, 2385–2397.
- 6 L. Zhuravlev, *Colloids and Surfaces A: Physicochemical and Engineering Aspects*, 2000, **173**, 1 – 38.